J. Phys. A: Math. Gen. 26 (1993) 5057–5069. Printed in the UK

Hierarchical analogues to fractional relaxation equations

H Schiessel and A Blumen

Theoretische Polymerphysik, Universität Freiburg, Rheinstr. 12, D-79104 Freiburg, Germany

Received 22 April 1993

Abstract. Recently fractional calculus has become an important tool in the analysis of slow relaxation phenomena, such as stress-strain relationships in polymeric materials. In the rheological constitutive equations this implies the replacement of the first-order derivatives by fractional derivatives. Here we show that such procedures have hierarchical mechanical analogues. We focus on the generalized dashpot and the generalized Maxwell model and display the corresponding arrangements. Our models allow a transparent interpretation of the parameters which enter the fractional equations, and reveal that the internal dynamics are hierarchically constrained.

1. Introduction

Relaxation processes in complex materials often display deviations from the exponential decay form [1, 2]. In addition to the stretched-exponential behaviour

$$\Phi(t) \propto \exp(-(t/\tau)^{\alpha}) \tag{1}$$

with $\alpha \in (0, 1)$, many materials show an algebraic decay

$$\Phi(t) \propto (t/\tau)^{-\gamma} \tag{2}$$

where $\gamma \in (0,1]$.

In the following, we restrict our considerations to the algebraic time-dependence (2) and related patterns. Such behaviour is observed for the stress relaxation of viscoelastic materials [3, 4], for charge-carrier transport in amorphous solids [5, 6], for the dielectric relaxation of liquids [7] and solids [8] and for current distributions at rough electrode–electrolyte interfaces [9, 10]. Although this work is formulated in viscoelastic terms, extensions of the following considerations to other physical situations are obvious.

A standard example for viscoelastic behaviour is the Maxwell model [11]. Consisting of a spring and a dashpot in series, this arrangement possesses a simple spatial separation of the solid (elastic) and the fluid (viscous) aspects. In this model the stress relaxation is exponential and thus the model is too special to describe real viscoelastic materials. As we proceed to show, arrangements of an (in general infinite) number of springs and dashpots lead to realistic forms such as equation (2).

A straightforward method for this would consist in arranging the Maxwell elements in parallel, so that their relaxation function is a sum of exponentials with different relaxation times. The physical picture behind such a procedure is that due to spatial inhomogenities in complex materials the relaxation times may vary from element to element. By a suitable choice of the weight distribution $\rho(\tau)$ of the spring constants E and viscosities η (and therefore the time constants $\tau=\eta/E$) the superposition

$$\Phi(t) \propto \int_0^\infty \rho(\tau) \exp(-t/\tau)\, d\tau \tag{3}$$

would mimic non-exponential patterns such as (1) and (2). However, such an approach is arbitrary on the microscopic level and therefore, it does not explain the universality of the measured patterns.

In this article we take another road. The starting point is the observation that *fractional calculus* is extremely useful for the mathematical description of the rheological behaviour of several classes of materials [4, 12, 13]. Replacing in the stress–strain relationship of the dashpot or the Maxwell model the first-order time derivatives (d/dt) by fractional derivatives (d^γ/dt^γ) of non-integer orders γ ($0<\gamma\leqslant 1$), equations of this type describe stress relaxation showing an algebraic decay (cf equation (2)) or more complicated patterns with crossover behaviour, respectively. The problem encountered by this approach, however, is that the expressions are rather formal and that no realizations of such abstract models are presented. Especially, no physical justification for the range of parameters is given.

In this work we present mechanical analogues for the generalized differential equations. The models are hierarchically built and consist of springs and dashpots. They simulate the generalized dashpot or the generalized Maxwell model to any given degree of accuracy and allow a lucid interpretation of the fractional rheological constitutive equations.

An analysis of the models reveals that their characteristic feature are *hierarchically constrained dynamics* in the sense of Palmer *et al.* [14], who studied the decay of coupled spin systems relaxing in a serial hierarchical fashion.

2. Fractional calculus and applications to viscoelasticity

The extension of classical calculus to its fractional counterpart can be most readily seen from a notation which unifies ordinary integration and differentiation:

$$\frac{d^\alpha f}{dt^\alpha}(t) = \begin{cases} f^{(\alpha)}(t) & \alpha=1,2,3,\ldots \quad (4a) \\ f(t) & \alpha=0 \quad (4b) \\ \int_0^t dt_{-\alpha-1} \int_0^{t_{-\alpha-1}} dt_{-\alpha-2} \ldots \int_0^{t_2} dt_1 \int_0^{t_1} f(t_0)\, dt_0 & \alpha=-1,-2,-3,\ldots \quad (4c) \end{cases}$$

together with the Riemann–Liouville integral [15]

$$\frac{d^\alpha f}{dt^\alpha}(t) = \frac{1}{\Gamma(-\alpha)} \int_0^t \frac{f(\tau)}{(t-\tau)^{\alpha+1}}\, d\tau. \tag{5}$$

For $\alpha=-1,-2,-3,\ldots$ one obtains namely Cauchy's formula for repeated integration [15] so that (4c) and (5) are equivalent. Now, the basic idea is that (5) can be readily extended to all $\alpha<0$. This defines *fractional integration*. Furthermore the domain of validity is extended to $\alpha>0$ by setting

$$\frac{\mathrm{d}^\alpha f}{\mathrm{d}t^\alpha}(t)=\frac{\mathrm{d}^n}{\mathrm{d}t^n}\left(\frac{\mathrm{d}^{\alpha-n}f}{\mathrm{d}t^{\alpha-n}}(t)\right) \tag{6}$$

where the integer n is chosen such that $n>\alpha$. Since definition (6) does not depend on n, one has thus defined the so-called *differintegration* of arbitrary order.

In the following, two properties of the fractional expressions are relevant: the composition rule and the behaviour under Laplace transformation. In general, the composition rule

$$\frac{\mathrm{d}^\beta}{\mathrm{d}t^\beta}\frac{\mathrm{d}^\alpha f}{\mathrm{d}t^\alpha}=\frac{\mathrm{d}^{\alpha+\beta}f}{\mathrm{d}t^{\alpha+\beta}} \tag{7}$$

is not valid. However, equation (7) holds for arbitrary values of β when restricted to the special class of differintegrable series (containing Taylor series) as long as $\alpha<0$; it holds even for $\alpha<1$ if f is bounded at $t=0$ [15].

The Laplace transform of a function f, $\bar{f}$, is defined through

$$\bar{f}(s)=\int_0^\infty \mathrm{e}^{-st}f(t)\,\mathrm{d}t \tag{8}$$

and one has for arbitrary α [15]

$$\overline{\frac{\mathrm{d}^\alpha f}{\mathrm{d}t^\alpha}}(s)=s^\alpha\bar{f}(s)-\sum_{k=0}^{n-1}s^k\frac{\mathrm{d}^{\alpha-1-k}f}{\mathrm{d}t^{\alpha-1-k}}(0) \tag{9}$$

where n is an integer chosen such that $n-1<\alpha\leqslant n$. Hence the sum vanishes for $n\leqslant 0$. Equation (9) is a generalization for Laplace transforms of integer-order derivatives and of multiple integrals and provides a convenient means to express fractional derivatives.

Differential equations with at least one derivative of non-integer order are called extraordinary differential equations [15]. In the following, two such relationships are used. As can be calculated from definition (6), the solution of the first one

$$g(t)=\frac{\mathrm{d}^\gamma f}{\mathrm{d}t^\gamma}(t) \tag{10}$$

with $\gamma\in(0,1)$ shows algebraic relaxation behaviour

$$g(t)=f_0\frac{t^{-\gamma}}{\Gamma(1-\gamma)}(t) \tag{11}$$

for a Heaviside-type input $f(t)=f_0\Theta(t)$.

Describing more complex relaxations (for example patterns which show crossovers) the following extraordinary differential equation is useful:

$$g(t)+\frac{\mathrm{d}^\alpha g}{\mathrm{d}t^\alpha}(t)=\frac{\mathrm{d}^\beta f}{\mathrm{d}t^\beta}(t) \tag{12}$$

with $0<\alpha\leqslant\beta\leqslant 1$. For given $f(t)=f_0\Theta(t)$, the Laplace transform of g simply fulfills (see equation (9))

$$\bar{g}(s)=f_0\frac{s^{\beta-1}}{1+s^{\alpha}}. \qquad (13)$$

Series expansion of (13) and termwise inverse transformation yield [13]

$$g(t)=f_0\Theta(t)\sum_{k=0}^{\infty}\frac{(-1)^k}{\Gamma(\alpha k+\alpha-\beta+1)}t^{\alpha-\beta+\alpha k}. \qquad (14)$$

The asymptotic behaviour

$$g(t)\propto\begin{cases}t^{\alpha-\beta} & \text{for } t\to 0\\ t^{-\beta} & \text{for } t\to\infty\end{cases} \qquad (15)$$

for $\beta<1$ follows for small t directly from (14), whereas the long-time behaviour can be derived from Tauberian theorems [16].

Rheological constitutive equations with fractional derivatives similar to (10) and (12) are very useful for describing the stress–strain relationship of polymers and other viscoelastic materials. The differential equation

$$\sigma(t)=\eta^{\gamma}E^{1-\gamma}\frac{\mathrm{d}^{\gamma}\varepsilon}{\mathrm{d}t^{\gamma}}(t) \qquad (16)$$

with $\gamma\in(0,1)$ is an interpolation between Hooke's law describing solid behaviour, i.e. $\gamma=0$

$$\sigma(t)=E\varepsilon(t) \qquad (17)$$

and Newton's law describing fluid behaviour, i.e. $\gamma=1$

$$\sigma(t)=\eta\frac{\mathrm{d}\varepsilon}{\mathrm{d}t}(t). \qquad (18)$$

In equations (17) and (18), E and η denote the spring constant and the viscosity, respectively.

After a strain jump $\varepsilon(t)=\varepsilon_0\Theta(t)$, we recover from (11) Nutting's law [3]:

$$\sigma(t)=\varepsilon_0\eta^{\gamma}E^{1-\gamma}\frac{t^{-\gamma}}{\Gamma(1-\gamma)}\Theta(t). \qquad (19)$$

The Maxwell model for viscoelasticity consists of a spring and a dashpot in series. As can be easily seen, the stress–strain relationship fulfills

$$\sigma(t)+\lambda\frac{\mathrm{d}\sigma}{\mathrm{d}t}(t)=\lambda E\frac{\mathrm{d}\varepsilon}{\mathrm{d}t}(t) \qquad (20)$$

with the relaxation time $\lambda=\eta/E$. Clearly, after a jump in the strain, the right-hand side (RHS) of (20) is proportional to a delta function and the stress relaxes exponentially. In recent years a series of works were devoted to describing more complex relaxation patterns by replacing in (20) the ordinary derivatives of stress and strain by fractional derivatives of orders α and β, respectively [4, 13, 17]:

$$\sigma(t)+\lambda^{\alpha}\frac{\mathrm{d}^{\alpha}\sigma}{\mathrm{d}t^{\alpha}}(t)=\lambda^{\beta}E\frac{\mathrm{d}^{\beta}\varepsilon}{\mathrm{d}t^{\beta}}(t). \qquad (21)$$

The discussion presented by Friedrich [13] about this stress–strain relationship, the so-called generalized Maxwell model, indicates that the behaviour of the solution is thermodynamically reasonable if the coefficients α and β obey $0<\alpha\leqslant\beta\leqslant 1$. Equation (21) interpolates between the usual Maxwell model (20) ($\alpha=\beta=1$) and Hooke's law (17) ($\alpha=\beta=0$). After a given strain jump $\varepsilon(t)=\varepsilon_0\Theta(t)$, the relaxation function of the stress fulfills (see equation (14))

$$\sigma(t)=\varepsilon_0\Theta(t)E\sum_{k=0}^{\infty}\frac{(-1)^k}{\Gamma(\alpha k+\alpha-\beta+1)}(t/\lambda)^{\alpha-\beta+\alpha k} \tag{22}$$

and shows therefore the asymptotic behaviour given in (15).

3. Mechanical analogues

We now proceed by first presenting a mechanical model (a generalization of the semi-integrating electrical circuit of [15] and its mechanical analogue, the so-called Gross–Marvin model [11]) and displaying the system of coupled linear differential equations which it fulfills. As we proceed to show, the system leads to continued-fraction expressions, which (in the limit of an infinite mechanical arrangement) are solutions of the fractional equation (10). In order to explain the current behaviour at an electrode–electrolyte interface, similar electrical models were constructed [18, 19]. However, these models were not related to fractional calculus. The arrangement of our model is shown in figure 1. It consists of a ladder-like structure with springs along one of the struts and dashpots on the rungs of the ladder. The following system of linear differential equations (23)–(26) describes the relationship between the stresses and the strains for all single structural parts of this finite arrangement. We denote by ε_k^s and ε_k^d the elongations of the spring E_k and the dashpot η_k, respectively, and choose

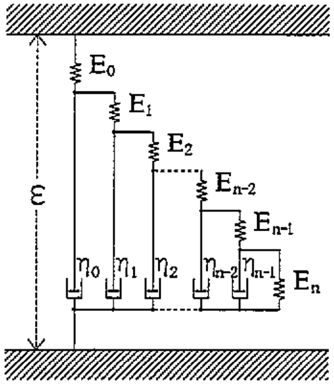

Figure 1. Diagram of the finite mechanical arrangement used to simulate the generalized dashpot (see text).

an analogous notation for the stresses. We note in particular:

(a) The additivity of the strains (as can be seen from the elongations)

$$\varepsilon_k^d=\varepsilon_{k+1}^s+\varepsilon_{k+1}^d \qquad k=0,1,\ldots,n-2 \tag{23a}$$

where the situation at the upper and the lower ends of this sections is

$$\varepsilon=\varepsilon_0^s+\varepsilon_0^d \tag{23b}$$

and

$$\varepsilon_{n-1}^d=\varepsilon_n^s. \tag{23c}$$

(b) The additivity of the stresses, due to the parallel arrangement:

$$\sigma_k^s=\sigma_{k+1}^s+\sigma_k^d \qquad k=0,1,\ldots,n-1 \tag{24a}$$

complemented by the situation at the end of the ladder

$$\sigma=\sigma_0^s. \tag{24b}$$

(c) Each structural part (dashpot or spring) obeys an equation analogous to (17)

$$\varepsilon_k^s=\frac{1}{E_k}\sigma_k^s \tag{25a}$$

or to (18)

$$\sigma_k^d=\eta_k\frac{\mathrm{d}\varepsilon_k^d}{\mathrm{d}t}. \tag{25b}$$

(d) Furthermore, causality implies that

$$\varepsilon(t\leqslant 0)=\sigma(t\leqslant 0)=0. \tag{26}$$

Now the aim is to get a relation between the Laplace transform of the elongation, $\bar{\varepsilon}$, and the Laplace transform of the stress, $\bar{\sigma}$. Combining equations (23*a*) and (25*a*), we obtain

$$E_{k+1}\bar{\varepsilon}_k^d(s)=\bar{\sigma}_{k+1}^s(s)+E_{k+1}\bar{\varepsilon}_{k+1}^d(s) \qquad k=0,1,\ldots,n-2. \tag{27}$$

Furthermore, using equations (24*a*) and (25*b*), we get, noting (9) for $\alpha=1$ and the initial condition (26)

$$\bar{\sigma}_k^s(s)=\bar{\sigma}_{k+1}^s(s)+s\eta_k\bar{\varepsilon}_k^d(s) \qquad k=0,1,\ldots,n-1 \tag{28}$$

from which it follows that

$$E_{k+1}\frac{\bar{\varepsilon}_k^d(s)}{\bar{\sigma}_{k+1}^s(s)}=1+E_{k+1}\frac{\bar{\varepsilon}_{k+1}^d(s)}{\bar{\sigma}_{k+1}^s(s)}=1+\cfrac{E_{k+1}/\eta_{k+1}}{s+\cfrac{1}{\eta_{k+1}}\cfrac{\bar{\sigma}_{k+2}^s(s)}{\bar{\varepsilon}_{k+1}^d(s)}}. \tag{29}$$

A special case is

$$E_{n-1}\frac{\bar{\varepsilon}_{n-2}^d(s)}{\bar{\sigma}_{n-1}^s(s)}=1+\frac{E_{n-1}/\eta_{n-1}}{s+E_n/\eta_{n-1}}. \tag{30}$$

Furthermore we also list the relation between $\bar{\sigma}_{n-2}^s$ and $\bar{\varepsilon}_{n-3}^d$:

$$\begin{aligned}E_{n-2}\frac{\bar{\varepsilon}_{n-3}^d(s)}{\bar{\sigma}_{n-2}^s(s)}&=1+\cfrac{E_{n-2}/\eta_{n-2}}{s+\cfrac{1}{\eta_{n-2}}\cfrac{\bar{\sigma}_{n-1}^s(s)}{\bar{\varepsilon}_{n-2}^d(s)}}\\&=1+\cfrac{E_{n-2}/\eta_{n-2}}{s+\cfrac{E_{n-1}/\eta_{n-2}}{1+\cfrac{E_{n-1}/\eta_{n-1}}{s+E_n/\eta_{n-1}}}}\end{aligned} \tag{31}$$

where (30) is used for establishing the equivalence on the RHS. After $n-2$ analogous steps we obtain

$$E_0\frac{\bar{\varepsilon}(s)}{\bar{\sigma}(s)}=1+\frac{s^{-1}\frac{E_0}{\eta_0}}{1+}\,\frac{s^{-1}\frac{E_1}{\eta_0}}{1+}\,\frac{s^{-1}\frac{E_1}{\eta_1}}{1+}\,\frac{s^{-1}\frac{E_2}{\eta_1}}{1+}\cdots\frac{s^{-1}\frac{E_{n-1}}{\eta_{n-1}}}{1+}\,\frac{s^{-1}\frac{E_n}{\eta_{n-1}}}{1} \tag{32}$$

a very convenient representation of the quotient $\bar{\varepsilon}(s)/\bar{\sigma}(s)$ as a continued fraction.

Now, the following relation holds for all $x>-1$ and real γ (equation (6.1.16) of [20]):

$$x(x+1)^{\gamma-1}=\frac{x}{1+}\,\frac{(1-\gamma)x}{1+}\,\frac{\frac{1\cdot(0+\gamma)}{1\cdot 2}x}{1+}\,\frac{\frac{1\cdot(2-\gamma)}{2\cdot 3}x}{1+}\,\frac{\frac{2\cdot(1+\gamma)}{3\cdot 4}x}{1+}\,\frac{\frac{2\cdot(3-\gamma)}{4\cdot 5}x}{1+}\cdots. \tag{33}$$

For $-1<x<1$ this can be easily seen by solving its terminating approximations; in this regime (33) corresponds to the binomial series (cf equation (3.6.8) of [21]). The RHS of (33) parallels now (32). Hence, choosing the parameters E_k and η_k such that

$$E_1/\eta_0=(1-\gamma)c_0 \qquad E_1/\eta_1=\frac{1\cdot(0+\gamma)}{1\cdot 2}c_0,\ \text{etc.} \tag{34}$$

with $c_0=E_0/\eta_0$, we obtain from (32)

$$E_0\frac{\bar{\varepsilon}(s)}{\bar{\sigma}(s)}=1+\frac{c_0/s}{1+}\frac{(1-\gamma)c_0/s}{1+}\cdots\frac{\frac{(n-1)(n-\gamma)}{(2n-1)(2n-2)}c_0/s}{1}. \tag{35}$$

As can be seen from (33), we get for $n\to\infty$

$$E_0\frac{\bar{\varepsilon}(s)}{\bar{\sigma}(s)}=1+(c_0/s)(c_0/s+1)^{\gamma-1}. \tag{36}$$

Given a preset $\delta(\delta\ll 1)$ one has for s small ($s<c_0\delta^{1/\gamma}$) the approximation

$$E_0\frac{\bar{\varepsilon}(s)}{\bar{\sigma}(s)}=(c_0/s)^{\gamma} \tag{37}$$

where the error in going from (36) to (37) is less than δ.

To display even better the domain of validity of (37) as an approximation to (35) we have plotted in figures 2 and 3 the quotient of the respective RHS. We have analysed the expression for several special cases and indeed found that (37) holds well (the relative error δ is smaller than 0.01), as long as the condition $c_0/s\in(100^{1/\gamma}, n^2/10)$ is obeyed. Here the upper bound is due to the truncation error of the continued fraction whereas the lower limit follows from the approximation of (36) by (37).

Thus, in this range we have to a very good approximation

$$\bar{\sigma}(s)=\eta_0^{\gamma}E_0^{1-\gamma}s^{\gamma}\bar{\varepsilon}(s). \tag{38}$$

Because of the boundary condition (26) we can read directly from (38) that its inverse Laplace transform (see equation (9)) obeys

$$\sigma(t)=\eta_0^{\gamma}E_0^{1-\gamma}\frac{d^{\gamma}\varepsilon}{dt^{\gamma}}(t) \tag{39}$$

for all t-values within the interval $(100^{1/\gamma}/c_0, n^2/(10c_0))$.

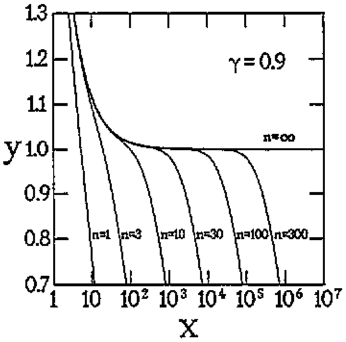

Figure 2. Comparison of the terminating continued fraction $E_0\bar{\varepsilon}(s)/\bar{\sigma}(s)$ of equation (35) with $(c_0/s)^{\gamma}$ for different values of n. The semilogarithmic plot shows $y=(E_0\bar{\varepsilon}(s)/\bar{\sigma}(s))/(c_0/s)^{\gamma}$ versus $x=c_0/s$ for $\gamma=0.9$.

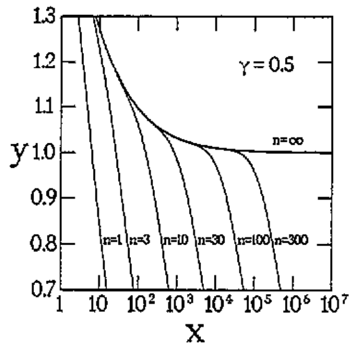

Figure 3. Same as figure 2, but $\gamma = 0.5$.

Hence in this range our mechanical analogue indeed fulfills the condition requested for the solution of our initial fractional expression, equation (16), if we choose the constants in such a way as to have

$$\eta_0^{\gamma} E_0^{1-\gamma} = \eta^{\gamma} E^{1-\gamma}. \tag{40}$$

We hasten to note that if we take the limit $n \to \infty$ in such a way that $\eta_0/E_0 = 1/n$ is obeyed we can extend the range of validity of (16) to all positive times.

Now a mechanical construction which obeys the generalized (fractional) Maxwell model, equation (21), is easily obtained. We show it in figure 4; it consists of a serial

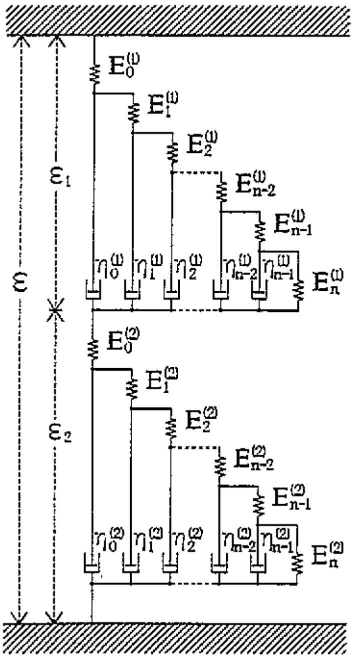

Figure 4. Diagram of the finite mechanical arrangement used to simulate the generalized Maxwell model (see text).

arrangement of two hierarchical systems. The strains of the two sections ($i=1$ and 2) are coupled through

$$\varepsilon=\varepsilon_1+\varepsilon_2 \tag{41}$$

whereas the stresses are equal:

$$\sigma=\sigma_1=\sigma_2. \tag{42}$$

If we choose the orders of differentiation as

$$\gamma_1=\beta-\alpha \qquad \gamma_2=\beta \tag{43}$$

the two sections fulfill

$$\sigma_1(t)=(\eta_0^{(1)})^{\beta-\alpha}(E_0^{(1)})^{1-\beta+\alpha}\frac{\mathrm{d}^{\beta-\alpha}\varepsilon_1}{\mathrm{d}t^{\beta-\alpha}}(t) \tag{44}$$

and

$$\sigma_2(t)=(\eta_0^{(2)})^{\beta}(E_0^{(2)})^{1-\beta}\frac{\mathrm{d}^{\beta}\varepsilon_2}{\mathrm{d}t^{\beta}}(t) \tag{45}$$

for all suitable t (cf equation (39)). Applying the operator $\mathrm{d}^\alpha/\mathrm{d}t^\alpha$ to both sides of (44) and using the composition rule (7) which holds since $\beta-\alpha<1$ and ε_1 is bounded at $t=0$, we obtain

$$\frac{\mathrm{d}^\alpha\sigma_1}{\mathrm{d}t^\alpha}(t)=(\eta_0^{(1)})^{\beta-\alpha}(E_0^{(1)})^{1-\beta+\alpha}\frac{\mathrm{d}^{\beta}\varepsilon_1}{\mathrm{d}t^{\beta}}(t). \tag{46}$$

Remembering now that $\varepsilon=\varepsilon_1+\varepsilon_2$ and $\sigma=\sigma_1=\sigma_2$ it follows from (45) and (46) that

$$(\eta_0^{(2)})^{-\beta}(E_0^{(2)})^{\beta-1}\sigma(t)+(\eta_0^{(1)})^{\alpha-\beta}(E_0^{(1)})^{\beta-\alpha-1}\frac{\mathrm{d}^\alpha\sigma}{\mathrm{d}t^\alpha}(t)=\frac{\mathrm{d}^\beta\varepsilon}{\mathrm{d}t^\beta} \tag{47}$$

as long as t obeys

$$\max_{i\in\{1,2\}}\{100^{1/\gamma_i}/c_0^{(i)}\}<t<\min_{i\in\{1,2\}}\{n^2/(10c_0^{(i)})\}$$

with $c_0^{(i)}=E_0^{(i)}/\eta_0^{(i)}$. Hence in this range our mechanical analogue indeed fulfills the condition requested for the fractional expression of the generalized Maxwell model, equation (21), if we choose the constants in such a way as to have

$$(\eta_0^{(2)})^{-\beta}(E_0^{(2)})^{\beta-1}=\lambda^{-\beta}E^{-1} \tag{48}$$

and

$$(\eta_0^{(1)})^{\alpha-\beta}(E_0^{(1)})^{\beta-\alpha-1}=\lambda^{\alpha-\beta}E^{-1}. \tag{49}$$

In the limit $n\to\infty$, such that $\eta_0^{(i)}/E_0^{(i)}=1/n$, the range of validity of (21) extends to all positive times.

In the following we consider several physical properties of this model. We focus first on the $E_k^{(i)}$ and $\eta_k^{(i)}$ which, using (34), obey the explicit forms

$$E_1^{(i)} = (1-\gamma_i)E_0^{(i)} \tag{50a}$$

$$E_k^{(i)} = \frac{k}{2k-1}\frac{\binom{k-\gamma_i}{k}}{\binom{k-2+\gamma_i}{k-1}}E_0^{(i)} \qquad k=2,3,\ldots n \tag{50b}$$

and

$$\eta_k^{(i)} = 2\frac{\binom{k-\gamma_i}{k}}{\binom{k-1+\gamma_i}{k}}\eta_0^{(i)} \qquad k=1,2,\ldots,n-1. \tag{50c}$$

In (50) the $\binom{x}{k}$ are generalized binomial coefficients

$$\binom{x}{k} = \frac{x(x-1)(x-2)\ldots(x-k+1)}{k!} = \frac{\Gamma(x+1)}{\Gamma(x+1-k)\Gamma(k+1)} \tag{51}$$

with $x \in IR$ and $k \in IN$.

Using Stirling's formula (equation (6.1.37) in [21])

$$\Gamma(x) \stackrel{x\to\infty}{\to} \sqrt{2\pi}x^{x-1/2}\,\mathrm{e}^{-x} \tag{52}$$

we get for the spring constants and viscosities the following algebraic k-dependence for large k:

$$E_k^{(i)} = \frac{E_0^{(i)}}{2}\frac{\Gamma(\gamma_i)}{\Gamma(1-\gamma_i)}k^{1-2\gamma_i} \tag{53}$$

and

$$\eta_k^{(i)} = 2\eta_0^{(i)}\frac{\Gamma(\gamma_i)}{\Gamma(1-\gamma_i)}k^{1-2\gamma_i}. \tag{54}$$

Now we are ready to discuss the implications of these expressions. We note first that the cases $\gamma_i<0$ and $\gamma_i>1$ lead for some k to negative values of $\binom{k-2+\gamma_i}{k-1}$ and $\binom{k-1+\gamma_i}{k}$ ($\gamma_i<0$) and $\binom{k-\gamma_i}{k}$ ($\gamma_i>1$). From (50*b*) and (50*c*) it follows that some spring constants and viscosities would become negative. Hence our model shows directly that the requirements $0\leqslant\gamma_1=\beta-\alpha\leqslant 1$ and $0\leqslant\gamma_2=\beta\leqslant 1$ are necessary to obtain positive values for $E_k^{(i)}$ and $\eta_k^{(i)}$ (cf equations (50*a*)–(50*c*)). According to [13], Friedrich has shown (by analysing the relaxation function) that the condition $0<\alpha\leqslant\beta\leqslant 1$ leads to thermodynamic compatibility. From our expressions we obtain the same relation for $\alpha>0$.

Moreover, as can be seen from (50*a*)–(50*c*), the case $\gamma_2=\beta=1$ leads to $E_k^{(2)}=\eta_k^{(2)}=0$ for all $k>1$ since then the terms $(1-\gamma_2)$ and $\binom{k-\gamma_2}{k}$ vanish. Therefore the lower hierarchy ($i=2$) is replaced by a simple Maxwell element and shows fluid-like behaviour. For $\gamma_2=\beta<1$ all spring constants are positive (cf equations (50*a*) and (50*b*)) and the arrangement figure 4 has an uninterrupted series of springs between its upper and lower ends. For that reason, the stress σ approaches infinity with increasing

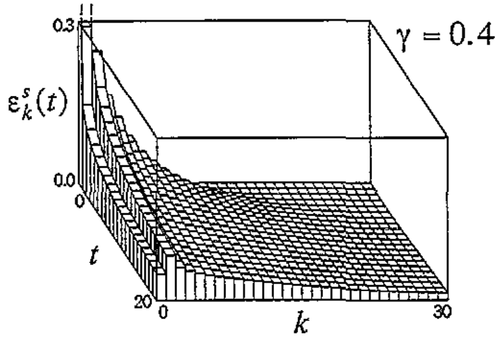

Figure 5. Internal dynamical behaviour of the one-ladder model figure 1. The plot shows $\varepsilon_k^s(t)$ versus t and k for $\gamma = 0.4$.

ε, and the model behaves in a solid-like manner. This is in accordance with [13], where Friedrich derived (by studying the asymptotic behaviour of the relaxation function) fluid-like behaviour of the fractional Maxwell model only in the case $\beta = 1$.

In the following we consider the internal dynamical behaviour of our model. We restrict the analysis to the one-ladder model with a finite n (cf equations (23)–(26) and figure 1). After a sudden strain jump $\varepsilon(t) = \varepsilon_0 \Theta(t)$, only the first spring E_0 is deformed ($\varepsilon_0^s = \varepsilon_0$) whereas the dashpot η_0 behaves in a rigid manner. The stress set up in the spring will gradually relax and fade away as the piston of the dashpot η_0 overcomes the resistance of the damping fluid. Simultaneously the spring in parallel, E_1, is deformed. In this way the deformation moves continuously into the ladder.

Now it is possible to understand how the special choice of the material constants controls the exponent γ of the algebraic decay of the stress $\sigma(t) \propto t^{-\gamma}$. As a function of the dependence of $E_k^{(i)}$ and $\eta_k^{(i)}$ on k, cf equations (53) and (54), the deformation moves slower or faster along the ladder. This then determines the temporal behaviour of the stress of the whole arrangement, $\sigma = \sigma_0^s$.

In order to give a feeling for the process which sets in after a Θ-pulsed strain of amplitude $\varepsilon_0 = 1$, we display two cases in figures 5 and 6. We set $\lambda = E = 1$ and take $n = 30$. The exponent γ varies between 0.4 and 0.8. The other constants are fixed by the conditions (40) and $\eta_0^{(i)}/E_0^{(i)} = 1/n$. The plots show $\varepsilon_k^s(t)$ versus t and k. As can be easily seen, for larger γ the deformation penetrates the ladder faster. The picture for small γ is in fact strongly reminiscent of the behaviour of photoconductive current under dispersive conditions [5].

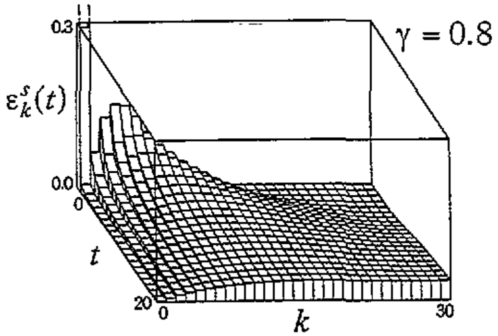

Figure 6. Same as figure 5, but $\gamma = 0.8$.

Summarizing, our model is an example of hierarchically constrained dynamics where the system relaxes in serial fashion.

4. Conclusions

In this work we have presented mechanical arrangements which permit simulation of the generalized dashpot and the generalized Maxwell model; from these arrangements some physical properties of the fractional rheological constitutive equations become evident by inspection. Thus, we have shown that the condition $0<\alpha\leqslant\beta$ required for the thermodynamic compatibility of the generalized Maxwell model translates here into the demand of positive viscosities and spring constants. Furthermore, the model shows fluid behaviour only for $\beta=1$, where one hierarchical ladder-arrangement gets replaced by a simple Maxwell element.

The basic features entering the mechanical models are hierarchically constrained dynamics, in line with the underlying physics of relaxation phenomena in many complex systems.

Acknowledgments

Fruitful suggestions and comments from professor C Friedrich are thankfully acknowledged. The work was supported by the SFB 60 of the DFG and by the Fonds der Chemischen Industrie.

References

[1] Klafter J, Rubin R J and Shlesinger M F (eds) 1986 *Transport and Relaxation in Random Materials* (Singapore: World Scientific)
[2] Blumen A, Klafter J and Zumofen G 1986 *Optical Spectroscopy of Glasses* ed I Zschokke (Dordrecht: Reidel)
[3] Nutting P G 1921 *Proc. Amer. Soc. Test. Mater.* **21** 1162
[4] Nonnenmacher T F 1991 *Rheological Modelling: Thermodynamical and Statistical Approaches* (Lecture Notes in Physics 381) eds J Casas-Vasquez and D Jou (Berlin: Springer)
[5] Scher H and Montroll E W 1975 *Phys. Rev.* B **12** 2455
[6] Schnörer H, Domes H, Blumen A and Haarer D 1988 *Phil. Mag. Lett.* **58** 101
[7] Cole K S and Cole R H 1941 *J. Chem. Phys.* **9** 341
[8] Jonscher A K 1977 *Nature* **267** 673
[9] Armstrong R D and Burnham R A 1976 *J. Electroanal. Chem.* **72** 257
[10] Bottelberghs P H and Broers G H J 1976 *J. Electroanal. Chem.* **67** 155
[11] Tschoegl N W 1989 *The Phenomenological Theory of Linear Viscoelastic Behavior* (Berlin: Springer)
[12] Smit W and de Vries H 1970 *Rheol. Acta* **9** 525
[13] Friedrich C 1991 *Rheol. Acta* **30** 151
[14] Palmer R G, Stein D L, Abrahams E and Anderson P W 1984 *Phys. Rev. Lett.* **53** 958
[15] Oldham K B and Spanier J 1974 *The Fractional Calculus* (New York: Academic)
[16] Feller W 1971 *An Introduction to Probability Theory and Its Applications* vol II (New York: Wiley)
[17] Giona M, Cerbelli S and Roman H E 1992 *Physica* **191A** 449
[18] Liu S H 1985 *Phys. Rev. Lett.* **55** 529
[19] Wang J C 1987 *J. Electrochem. Soc.* **134** 1915
[20] Jones W B and Thron W J 1980 *Continued Fractions* (London: Addison-Wesley)
[21] Abramowitz M and Stegun I A (eds) 1972 *Handbook of Mathematical Functions* (New York: Dover)